Tribology Letters (2022) 70:100
https://doi.org/10.1007/s11249-022-01637-9

ORIGINAL PAPER

Tribological Behavior of a Shot-Peened Nickel-Based Single Crystal Superalloy at High Temperature

Shouyi Sun[1,2] · Lei Li[1] · Chuanyun Hu[1] · Qi Li[3] · Tianyu Yuan[1]

Received: 11 May 2022 / Accepted: 28 July 2022 / Published online: 22 August 2022

Abstract

The tribological behavior of a nickel-based single crystal superalloy treated by shot-peening has been investigated. Friction tests under three normal loads and three temperatures were carried out based on the ball-on-disk configuration. The results showed that coefficient of friction (COF) and wear rate of the shot-peened nickel-based single crystal superalloy (SP-NBSC) at room temperature were nearly 2 times and 4 times that at 600 ℃, respectively. However, there were no significant differences in COF and wear rate between the SP-NBSC superalloy and the as-received NBSC superalloy, which was ascribed to the competing effects between the increased hardness and roughness of the SP-NBSC superalloy. High-temperature friction promoted the formation of a glaze-layer on the substrate, which was derived from the sintering and compacting of the wear debris. The formed glaze-layer prevented the direct contact of the friction pair and contributed to the reduced COF and wear rate. The wear mechanism of the SP-NBSC superalloy at high temperature including oxidation, adhesion, and abrasion. With the decreasing normal load and increasing temperature, the adhesive wear weakened. This work provided insights into the effects of shot-peening treatment on the tribological properties of the NBSC superalloy.

✉ Lei Li
lileinpu@nwpu.edu.cn

✉ Qi Li
Liqi801@163.com

[1] Department of Engineering Mechanics, Northwestern Polytechnical University (Chang'an Campus), Xi'an 710129, People's Republic of China

[2] State Key Laboratory of Tribology, Tsinghua University, Beijing 10084, People's Republic of China

[3] ENN Energy Power Technology (Shanghai) Co., Ltd, Shanghai 201306, People's Republic of China

Graphical Abstract

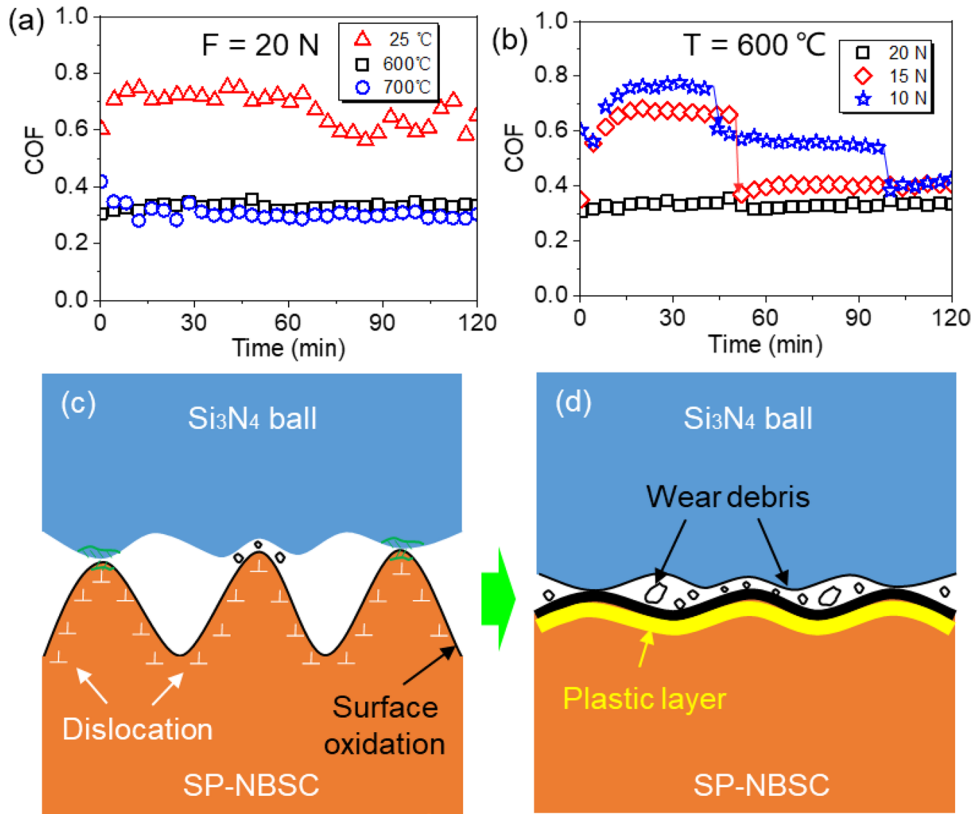

Keywords Shot-peening · Nickel-based single crystal · Tribological performance · High temperature · Glaze-layer

1 Introduction

Wear affects the operation of mechanical systems at high temperature, such as the bearings and the blade-disk assemblies in aero-engines and gas turbines [1, 2]. High-temperature wear causes the deterioration of structural surface and the variation of contact status, which has become one of the life-limiting factors of high-temperature components [3, 4]. Nickel-based single crystal (NBSC) superalloys were preferred in turbine blades due to their excellent mechanical properties at high temperature [5]. To meet the requirement of high-performance aero-engines and gas turbines, the NBSC turbine blades were typically strengthened by shot-peening treatment to improve their anti-fatigue performance, which were attributed to the introduction of favorable compressive residual stress and deep work hardening zone [6, 7]. However, the tribological behavior of the shot-peened nickel-based single crystal (SP-NBSC) superalloy has not been investigated at high temperature.

Shot-peening treatment can result in the fine grain microstructure and large surface hardness, but also increase the surface roughness [8]. The change of the mechanical properties and surface morphologies caused by shot-peening treatment would have a great influence on the tribological properties of materials. It has been reported that shot-peening treatment can improve the wear resistance and fatigue

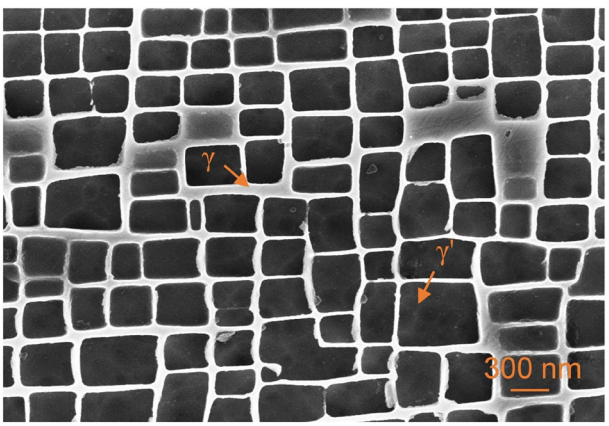

Fig. 1 Microstructure of the NBSC superalloy. The black region indicates the γ' precipitate phases, and the gray region represents the γ matrix phase

Table 1 The major chemical composition and element percentage of the NBSC superalloy (wt%)

Element	C	Cr	Co	W	Mo	Al	Re	Ta	Ni
wt%	≤0.04	3.8–4.8	8.5–9.1	7.0–9.0	1.5–2.5	5.2–6.2	1.6–2.4	6.0–8.5	Bal

life mainly by introducing high compressive residual stress and large hardness in the depth direction [9–11]. Nevertheless, in some cases, shot-peening treatment has no effects or even opposite effects on the tribological behaviors of alloys. Zammit et al. [12] found that the effects of microstructure transformation and compressive residual stress on the tribological behavior of the iron were counteracted, and no improvement of wear resistance was observed. Besides, shot-peening showed no effect on the wear behavior of Ti6Al4V alloy under fretting loading [13]. Tribological behavior of materials after shot-peening treatment mainly depended on the surface microstructure, residual stress field, and surface morphology. Moreover, the microstructure and residual stress field were also affected by the elevated temperature, which need to be probed to reveal the influencing mechanism of the shot-peening treatment on the tribological performance.

High-temperature wear process includes oxidation, creep, fatigue, and frictional effects, among which the dramatically change of the physical, chemical, and mechanical properties will directly affect the tribological behavior [14, 15]. During the friction process of nickel-based superalloy at high temperature, it has been found that a thin and physically homogeneous oxide layer was formed on the component surface [16–19]. The formed oxide layer was also known as the glaze-layer, which was reported to contribute to the low coefficient of friction (COF) and low wear rate for NBSC superalloys at high temperature [20, 21]. A widely recognized speculation was that the glaze-layer was formed by compacting and sintering the wear particles produced during the sliding process with the presence of heat [17, 22, 23]. The glaze-layer prevented the direct contact between the friction pair, therefore, the properties of the glaze-layer would directly influence the tribological behaviors of the superalloys at high temperature [24]. Moreover, it was reported that the formation of the glaze-layer was affected by the contact load and temperature. On the one hand, the lower contact load could not destroy the surface oxide film, while the larger contact load would break the glaze-layer excessively and prevent it from forming [25]. On the other hand, the glaze-layer formed only when the environmental temperature reached the certain threshold [26].Therefore, it was important to investigate the formation of the glaze-layer on the SP-NBSC superalloys to reveal the wear mechanism.

NBSC superalloys contained many doping elements, such as chromium, cobalt, tungsten etc., which resulted in complex tribo-reaction during the friction process at high temperature. For the nickel-based alloys, it was found that the friction promoted the formation of NiO phase, which was an effective lubricous binary oxide [27, 28]. Chromium can easily react with oxygen and form Cr_2O_3, which was known for its favorable tribological characteristics due to the excellent resistance to particles fracture and micro-cracks [17, 29]. In comparison with nickel oxides and chromium oxides, cobalt oxides have been reported to have lower friction and less wear, and they preferred to form a continuous solid film instead of being worn off [21, 30]. WO_3 with a high content will make the glaze-layer porous, that was inconducive for wear reduction [29]. Al_2O_3 owned strong ionic/covalent bonds that were difficult to shear and beneficial to the wear resistance [28]. Generally, friction-induced glaze-layer at high temperature comprised different kinds of oxides, and analyzing the composition of the glaze-layer would be conducive to the further analysis of the tribological behavior of the SP-NBSC superalloy.

In the present study, the tribological behavior of an SP-NBSC superalloy was investigated. Friction tests under different temperatures and normal loads were carried out to study the evolution of COF and wear rate. The morphologies and chemical compositions of the wear track on the SP-NBSC superalloy were characterized to study the wear damage and the formation of the glaze-layer. Furthermore,

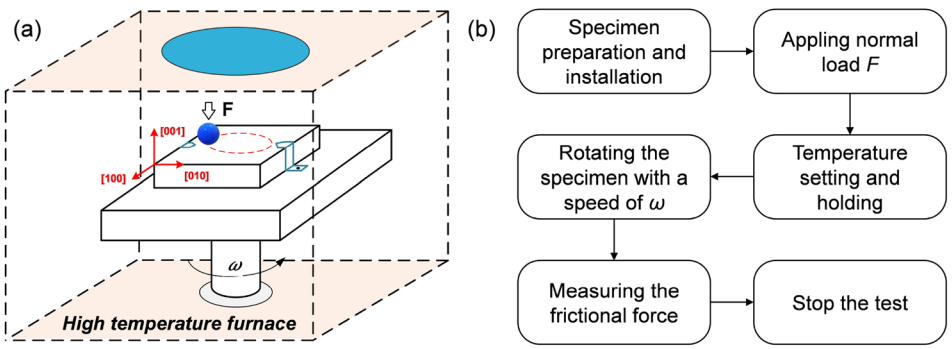

Fig. 2 The illustration of the high-temperature friction test. **a** The schematic of ball-on-disk friction test at high temperature, and **b** the flowchart of the high-temperature friction test

the cross-sectional morphologies of the wear scars were also analyzed to further reveal the characteristics of the formed glaze-layer between the friction pairs. Based on the analysis results, the feasible wear mechanism of the SP-NBSC superalloy was proposed, which provided support for understanding the tribological behavior of NBSC superalloys after shot-peening treatment.

2 Materials and Methods

2.1 Materials and Specimen

An NBSC superalloy DD6, which was typically applied in aero-engine turbine blades, was treated by shot-peening for the friction tests. The microstructure of the NBSC superalloy consisted of a large volume fraction of $L1_2$ ordered γ' precipitates coherently embedded in the faced centered cubic γ matrix (Fig. 1). NBSC superalloy contained a variety of metal elements, and the major chemical compositions of the DD6 superalloy are shown in Table 1. The NBSC specimen was processed into the square plate ($20\times20\times4$ mm^3) using wire electrical discharge machining, and the surface roughness was about 0.8 μm after polishing. The [001] crystal orientation of the NBSC superalloy was in consistence with the thickness direction of the specimen. Cast steel ball with a 0.3 mm diameter was used as the projectile to shot the specimen surface, and the shot-peening intensity was about 0.165 mmA, which can effectively improve the fatigue resistance of the NBSC superalloy.

2.2 Friction Test

To investigate the tribological behavior of the SP-NBSC superalloy at high temperature, friction tests were performed using a high-temperature tribometer (HT-1000) with a rotation mode based on the ball-on-disk configuration (Fig. 2a). The upper specimen was a Si_3N_4 ball with a diameter of 6 mm, which had high hardness and excellent wear resistance [31]. Besides, the property of Si_3N_4 was stable at high temperature that will not affect the evolution of the SP-NBSC superalloy during the friction process [32]. Before each test, the SP-NBSC superalloy specimen and the Si_3N_4 ball were supersonically cleaned with acetone and alcohol in sequence for 30 min to remove the surface contamination. The rotational angular velocity of the SP-NBSC specimen was 560 rpm with a constant rotation radius of 5 mm. Friction tests with three different normal loads varying from 10 to 20 N were carried out to study the effects of normal load on the tribological behavior of the SP-NBSC superalloy (the corresponding maximum Hertz contact stress varied from 1.27 to 1.60 GPa). Besides, the friction tests were performed at three representative temperatures (25, 600, and 700 ℃), which corresponded to the actual operation condition of the blade-disk assembly [25]. During the high-temperature friction test, the specimen was fixed in the furnace, which was then heated to the preset temperature and hold for 20 min to ensure the uniformity of the test temperature (Fig. 2b). The friction tests under different test conditions were repeated twice to ensure the accuracy, and each test was carried out for 120 min.

2.3 Characterization

A three-dimensional integral microscopy with enhanced resolution and depth of field (KEYENCE, VHX-700FC) was used to observe the surface morphologies of the SP-NBSC superalloy before and after the friction tests. The surface harnesses of the SP-NBSC superalloy and the as-received nickel-based single crystal (AS-NBSC) superalloy were measured using a microhardness tester (Qness Q60A+). Moreover, the surface hardnesses of the wear scars on the SP-NBSC superalloy after the friction tests were measured using a Nanoindentation system (Keysight G200), and the maximum applied load, loading rate, and holding time at the maximum load before unloading

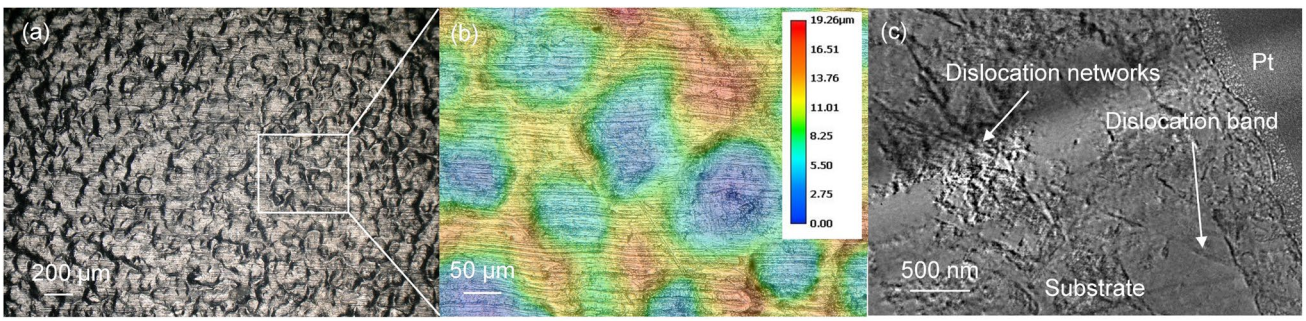

Fig. 3 The characterization of the SP-NBSC superalloy. **a** The surface morphology of the SP-NBSC superalloy. **b** The contour plot of the three-dimensional profile of the SP-NBSC superalloy. **c** TEM morphology of the shot-peened region of the SP-NBSC superalloy beneath the surface

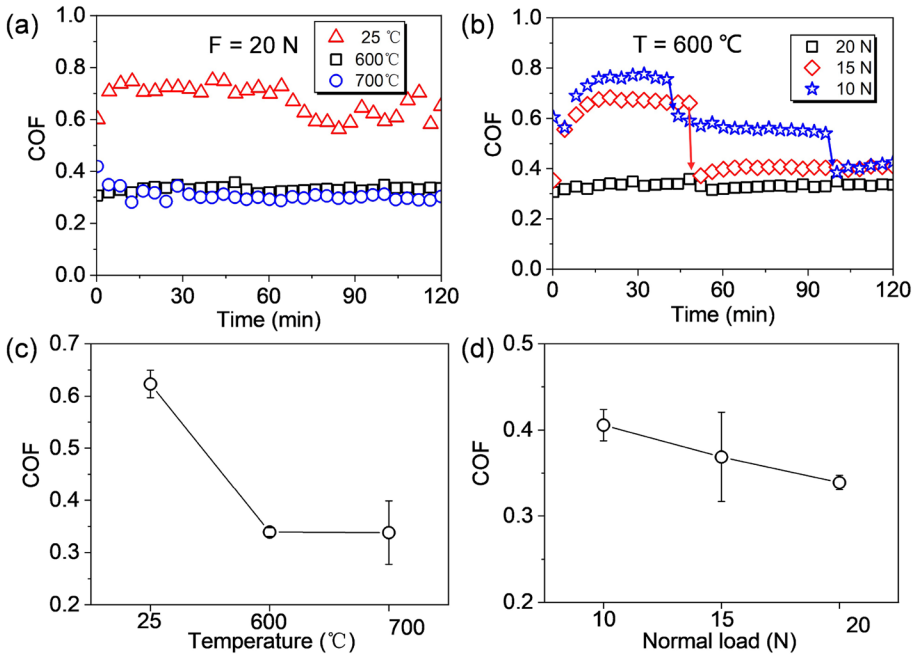

Fig. 4 COF of the Si_3N_4/SP-NBSC superalloy friction pair under different test conditions. **a** The evolutions of COF under different test temperatures with a constant normal load of 20 N. **b** The evolutions of COF under different normal loads when the test temperature was 600 ℃. **c** The averaged COF under different test temperatures with a constant normal load of 20 N. **d** The averaged COF under different normal loads at 600 ℃

were 50 mN, 3.3 mN/s, and 10 s, respectively. A Raman spectrometer (Thermo Scientific DXR2) with a laser wavelength of 532 nm was used to identify the chemical compositions of the worn regions. Besides, a scanning electron microscopy (SEM) (FEI, Verios G4) equipped with an energy-dispersive spectrometer (EDS) was applied to investigate the microstructures and chemical compositions of the wear tracks on the SP-NBSC superalloy. The cross-sectional morphology of the shot-peened region of the SP-NBSC superalloy was observed using a high-resolution transmission electron microscopy (HRTEM, 2100plus, Jeol, Japan).

Wear rate was an important factor to evaluate the tribological performance of the moving assembly, which can be quantified as the volume of material removed by the counterpart normalized by the normal load and the sliding distance [28]. After the friction test, the wear volume was calculated as the product of the averaged cross-sectional area and circumference of the wear track, as shown in Eq. (1)

$$V = 2\pi RS\,, \tag{1}$$

where R was the rotation radius and S was the averaged cross-sectional area of the wear track, which was obtained using the three-dimensional integral microscopy. The wear rate can be calculated as follows:

$$W_{\mathrm{r}} = \frac{V}{FL}, \tag{2}$$

where W_{r} indicated the wear rate, V was the wear volume, F and L were the applied normal load and the sliding distance, respectively.

3 Results and Discussion

3.1 Characterization of the SP-NBSC Superalloy

Shot-peening treatment caused the change of microstructure and surface morphology. The surface morphology of the SP-NBSC superalloy was observed by the three-dimensional integral microscopy (Fig. 3a). It can be found that many impact pits were distributed on the specimen surface induced by the steel balls with high speeds. The enlarged morphology showed that the impact pits seemed like irregular circles with an averaged depth of about 20 μm (Fig. 3b). The surface roughness of the SP-NBSC superalloy was about 9.35 μm, which was more than ten times that of the AS-NBSC superalloy. The increased surface roughness indicated that the serious plastic deformation occurred on the specimen surface. Moreover, the microstructure of the cross-sectional region near the shot-peened surface showed that shot-peening treatment introduced dislocation bands and dislocation networks beneath the surface (Fig. 3c). Shot-peening treatment improved the surface hardness of the NBSC superalloy from 370 to 551 Hv, and the improvement of the surface harness was mainly attributed to the severe plastic deformation and strain hardening [33].

3.2 Tribological Performance

To investigate the tribological performance of the SP-NBSC superalloy, the friction tests under different temperatures and normal loads were carried out. It can be observed that the

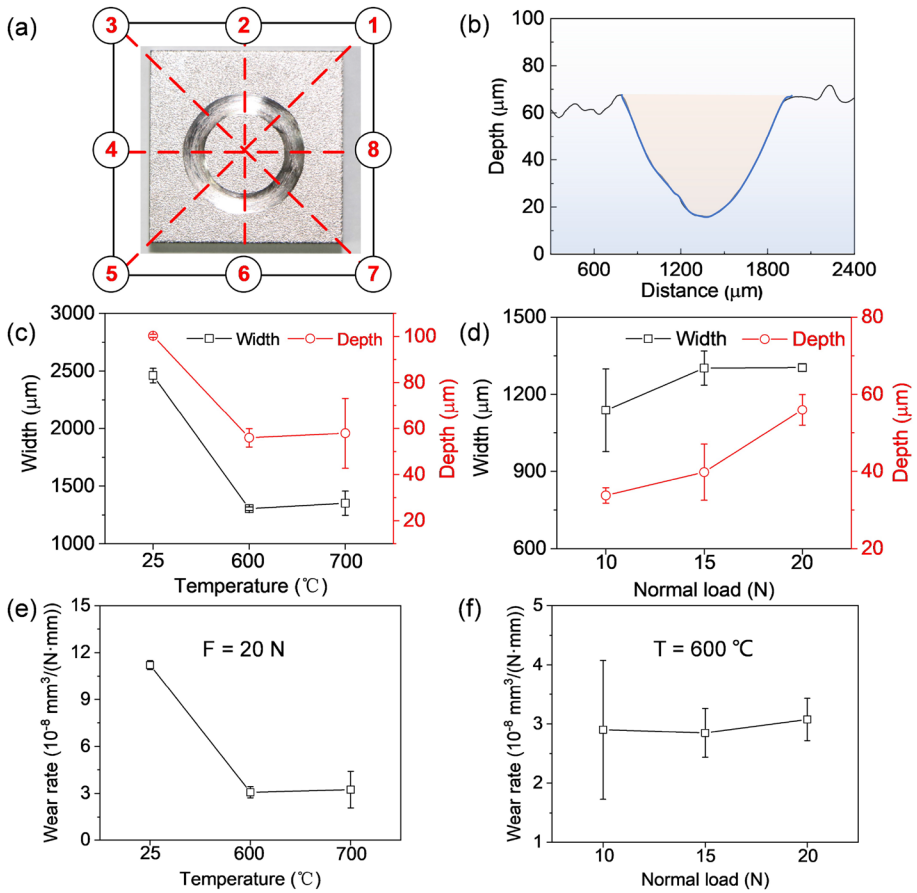

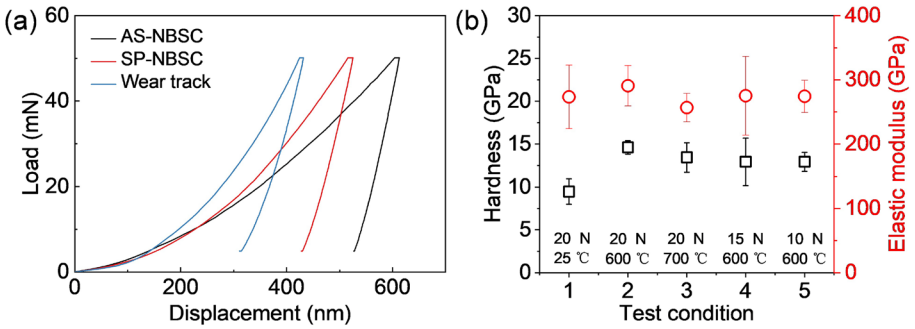

Fig. 5 **a** The surface morphology and **b** the cross-sectional morphology of the wear scar on the SP-NBSC superalloy after the friction test (the normal load and test temperature were 20 N and 600 ℃, respectively). **c** The widths and depths of the wear tracks at different test temperatures under the constant normal load of 20 N. **d** The widths and depths of the wear tracks under different normal loads at 600 ℃. **e** Wear rates of the SP-NBSC superalloy at different test temperatures under the constant normal load of 20 N. **f** Wear rates of the SP-NBSC superalloy under different normal loads at 600 ℃.

Fig. 6 **a** The representative nanoindentation curves of the AS-NBSC superalloy, the SP-NBSC superalloy, and the wear track on the SP-NBSC superalloy after the friction test (the applied normal load and test temperature were 20 N and 600 ℃, respectively). **b** The nanohardness and elastic modulus of the wear track on the SP-NBSC superalloy after different test conditions

COF evolutions under different test temperatures exhibited dramatical differences (Fig. 4a). At room temperature (about 25 ℃), the initial COF reached to about 0.7 and lasted for about 60 min, and then decreased to about 0.6. When the temperature increased to 600 or 700 ℃, the corresponding COF during the steady wear period was more stable and about half of that at room temperature, it can be deduced that high temperature promoted the tribo-chemical reaction that was beneficial to friction reduction. Besides, the averaged COFs during the steady wear period decreased with the increase of test temperature, but there was little difference in COF when the test temperatures were 600 and 700 ℃ (Fig. 4c). However, the evolution of COF showed great difference under different normal loads at 600 ℃ (Fig. 4b). It can be observed that when the normal load was 15 N, the COF increased to about 0.65 rapidly and lasted for about 30 min, and then, it decreased to about 0.4 sharply. The larger COF during the running-in period at 15 N may be

resulted from the instability of the formed glaze-layer under lower normal load. With the continuous sliding, the COF would decrease finally, which indicated that the stable glaze-layer was formed. Similarly, when the normal load was 10 N, the evolution of COF also exhibited the characteristics of piecewise decline. It can be deduced that larger normal load promoted the formation of stable tribo-layer. Moreover, the averaged COF increased from 0.3 to 0.4 when the normal load decreased from 20 to 10 N (Fig. 4d). Therefore, it can be concluded that both temperature and normal load had a great influence on COF. Besides, the averaged COFs of the SP-NBSC superalloy under different test conditions showed no great differences compared with those of the AS-NBSC superalloy, which may be due to the competing effects between the high hardness and the large roughness [25].

After the friction tests, the morphologies of the wear track on the SP-NBSC superalloy were analyzed. The macroscopic morphology of a representative wear scar showed that an annular trace formed on the specimen surface after the friction test (Fig. 5a). To analyze the characteristics of the wear tracks quantitatively, the cross-sectional morphologies were measured by using the three-dimensional integral microscopy at eight different locations (marked in Fig. 5a). The cross-sectional morphology at a representative location is shown in Fig. 5b, and the circular profile was ascribed to the uneven distribution of contact stresses according to the Hertz theory. When the normal load was 20 N, both the widths and depths of the wear tracks were lower at 600 and 700 ℃ compared with those at room temperature, which indicated that high temperature promoted the wear reduction (Fig. 5c). Besides, the depths of the wear tracks increased when the normal load increased from 10 to 20 N at 600 ℃, but the widths of the wear tracks did not change too much when the normal load varied from 15 to 20 N (Fig. 5d). For all the friction tests, the depths of the wear scar were all greater than 35 μm, which were larger than the thickness of the plastic layer induced by shot-peening treatment. Therefore, it can be inferred that the shot-peening-induced plastic layer has been worn out after 2 h of friction tests.

The wear rates of the SP-NBSC superalloy under different test conditions were calculated to further investigate its tribological performance. It could be observed that the wear rate of the SP-NBSC superalloy was about 11.21×10^{-8} $mm^3/(N \cdot mm)$ at room temperature, which was almost three times those at 600 ℃ and 700 ℃. Besides, the wear rate of the SP-NBSC superalloy at 700 ℃ was about 20% higher than that at 600 ℃, which may be due to the deterioration of the mechanical properties at higher temperature. Moreover,

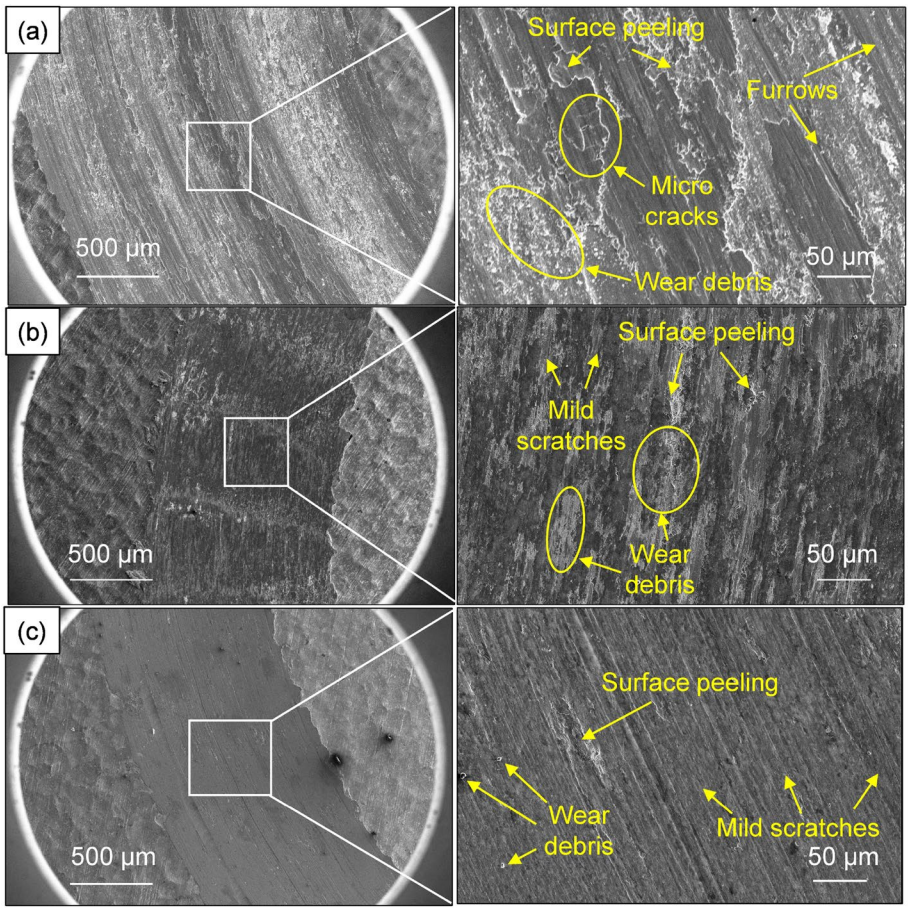

Fig. 7 SEM morphologies of the wear tracks on the SP-NBSC superalloy under different test temperatures when the normal load was 20 N. **a** Room temperature, **b** 600 ℃, and **c** 700 ℃

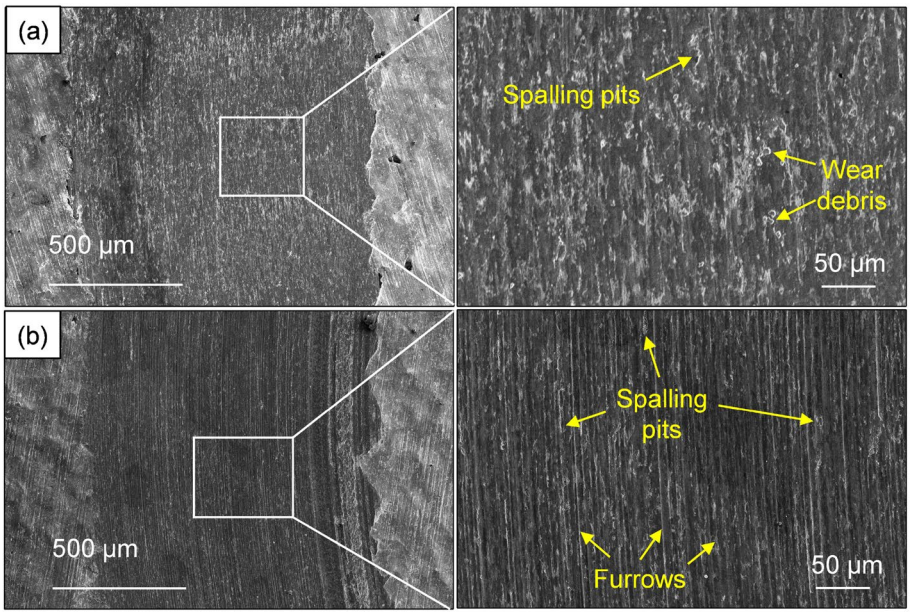

Fig. 8 SEM morphologies of the wear tracks on the SP-NBSC superalloy under different normal loads when the test temperature was 600 ℃. **a** 15 N and **b** 10 N

Table 2 The element percentage of the wear scar under different test conditions (wt%)

Test condition F/T	C	O	Al	Cr	Co	Ni	W
20 N/25 ℃	10.76	4.34	5.21	6.41	9.52	59.21	4.55
20 N/600 ℃	6.41	19.93	4.54	5.54	8.00	49.68	5.90
20 N/700 ℃	4.27	19.94	5.05	6.13	8.86	49.90	5.85
15 N/600 ℃	2.95	21.10	4.84	5.47	10.67	51.58	3.39
10 N/600 ℃	3.45	18.98	4.95	5.26	9.25	55.51	2.60

the wear rates showed little difference when the normal load varied from 10 to 15 N, but the wear rate increased as the normal load increased to 20 N, which was consistent with the results of the AS-NBSC superalloy [25]. In summary, although shot-peening treatment resulted in the increased surface roughness, the wear rate of the SP-NBSC superalloy showed little difference in comparison with the AS-NBSC superalloy, and the decreased wear rate at high temperature may be ascribed to the formed glaze-layer during the friction process.

3.3 Analysis of the Wear Scar

The tribological behavior of the SP-NBSC superalloy showed great difference under different test conditions, which could lead to distinguished wear damage. To investigate the mechanical properties of the wear scar after the friction tests, the nanoindentation tests were carried out. Before the friction test, it can be found that the representative nanoindentation curves of the AS-NBSC superalloy and the SP-NBSC superalloy showed great difference (Fig. 6a), and the surface nanohardness increased from 6.25 to 10.20 GPa after the shot-peening treatment, which was

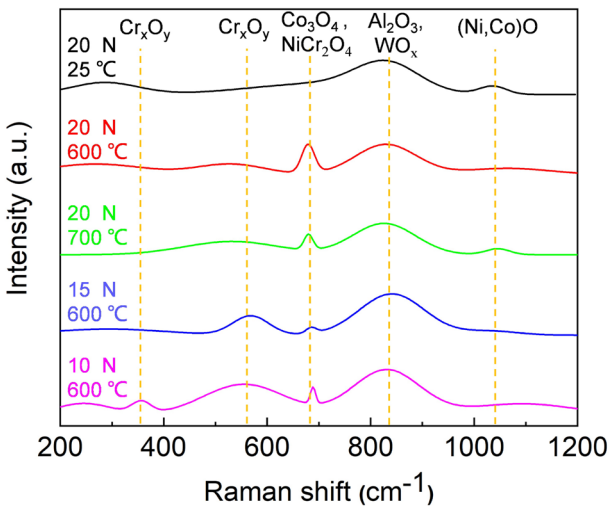

Fig. 9 Raman spectra of the worn regions under different test conditions

in consistence with the results of the microhardness tests. Besides, the elastic modulus of the SP-NBSC superalloy was 274.00 GPa, which was about 17.6% higher than that

of the AS-NBSC superalloy. However, after the friction test, the nanohardness of the wear track on the SP-NBSC superalloy changed significantly. When the applied normal load was 20 N and the test temperature was 600 ℃, the measured nanohardness and elastic modulus were 14.61 GPa and 290.73 GPa, respectively. The increased nanohardness and elastic modulus were ascribed to the strain hardening and the formation of high-temperature triggered metal oxides [34–36]. Moreover, when the applied load decreased to 15 N and 10 N, both the nanohardnesses of the wear scars were about 12.93 GPa, and the elastic moduli were 275.12 GPa and 274.32 GPa, respectively (Fig. 6b). The decreased nanohardness and elastic modulus under the lower applied load might attribute to the weaker strain hardening. As the test temperature increased to 700 ℃, the nanohardness and elastic modulus of the wear track were 13.45 GPa and 256.68 GPa, respectively. The lower nanohardness and elastic modulus compared with those at 600 ℃ were probably due to the different strain-hardening behavior at higher temperature. Overall, the increased nanohardness of the wear scar after the high-temperature friction test was beneficial to the wear resistance of the SP-NBSC superalloy.

To explore the effects of temperatures and loads on the wear damage, the morphologies of the wear tracks on the SP-NBSC superalloy were investigated using SEM. It could be found that some micro-cracks were distributed on the surface of SP-NBSC superalloy after the friction test at room temperature (Fig. 7a), and severe surface peeling occurred due to the high contact stress. Besides, there were many flake-like wear debris attached to the specimen surface, and some deep furrows were generated. It can be inferred that adhesive and abrasive wear was the main wear mechanism for the SP-NBSC superalloy at room temperature. As the test temperature increased to 600 ℃, the surface material was heavily oxidized, and parts of the oxides were worn off and crushed into fine wear debris (Fig. 7b). The wear track was smoother compared with that at room temperature, which exhibited the typical characteristic of glaze-layer [37]. Besides, some mild scratches were also distributed on the specimen surface. It can be deduced that the SP-NBSC superalloy underwent more severe abrasive wear at 600 ℃ than that at room temperature. When the test temperature was 700 ℃, the surface morphologies of the wear track showed different characteristics, which was smoother than those at room temperature and 600 ℃ (Fig. 7c). The formed oxides on the specimen surface seemed dense, and mild scratches were formed on the specimen surface with little granular wear debris attached. Therefore, the abrasive wear was the main wear mechanism when the temperature increased to 700 ℃.

Furthermore, the effects of normal loads on the wear damage of the SP-NBSC superalloy at 600 ℃ were also investigated. When the normal load was 15 N, some spalling pits can be observed on the wear track, which was mainly

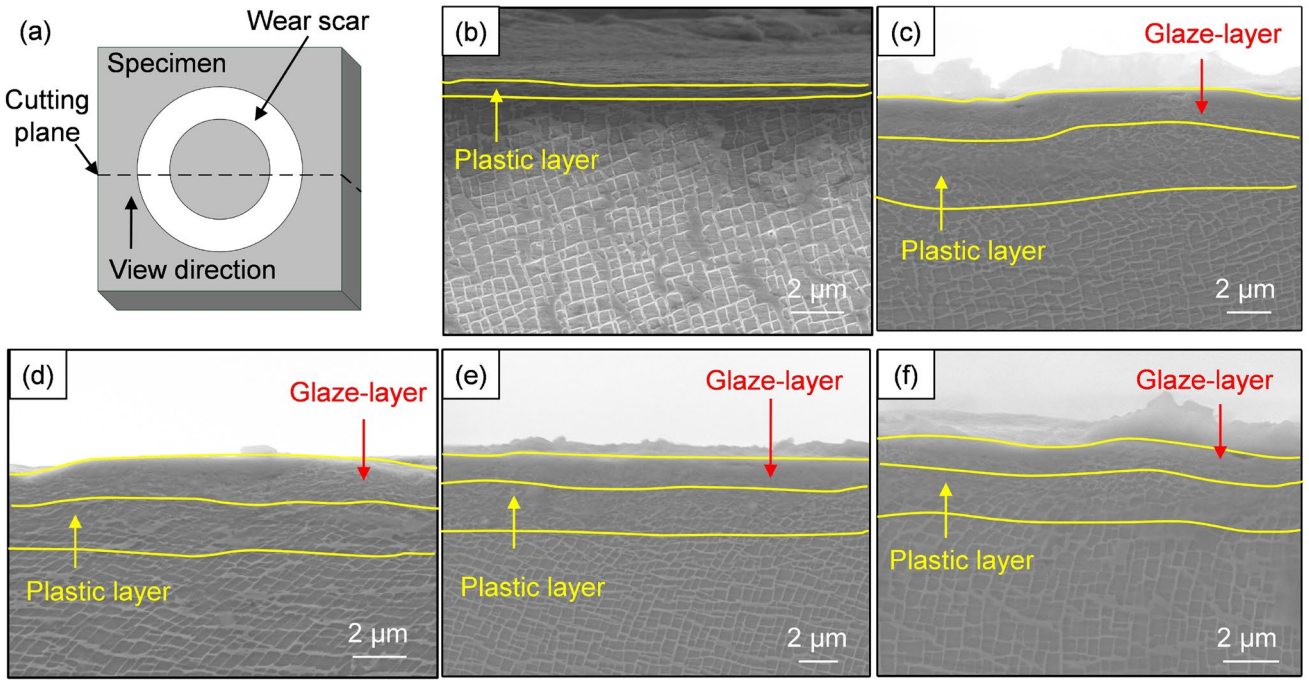

Fig. 10 **a** The schematic diagram of the SP-NBSC superalloy specimen after the friction test. The cross-sectional SEM morphologies of the wear scars under test condition of **b** $F=20$ N, $T=25$℃, **c** $F=20$ N, $T=600$ ℃, **d** $F=20$ N, $T=700$ ℃, **e** $F=15$ N, $T=600$ ℃, and **f** $F=10$ N, $T=600$ ℃

induced by the large frictional stress (Fig. 8a). Then, the materials removed from the surface will be crushed into fine wear debris under the action of high contact stress. After the friction test, it can be found that some flake-like wear debris were retained on the worn region. As the normal load decreased to 10 N, many shallow furrows were observed on the wear track, and the direction of the furrows was consistent with the sliding direction (Fig. 8b). Besides, there were some elongated spalling pits near the furrows. It can be deduced that the abrasive wear became the main wear mechanism when the normal load decreased from 20 to 10 N.

It has been reported that the formed glaze-layer during high-temperature friction process promoted the reduction of COF and wear rate. Therefore, the chemical composition of the glaze-layer under different test conditions was investigated using EDS, and the element percentage in the wear track is shown in Table 2. It can be found that the contents of oxygen were almost 20% when the test temperature was 600 ℃ and 700 ℃, while the content of oxygen was 4.34% after the friction test at room temperature. It can be deduced that both the friction-induced heat and the high-temperature environment promoted the surface oxidation during the high-temperature friction process. The composition of the formed oxides would have a great influence on the tribological performance of the SP-NBSC superalloy.

To further analyze the material composition of the glaze-layer, Raman spectra analyses under different test conditions were performed, as shown in Fig. 9. There were nearly five different peaks located at 360 cm^{-1}, 550 cm^{-1}, 680 cm^{-1}, 830 cm^{-1}, and 1060 cm^{-1}, respectively. The strongest peak appeared at around 830 cm^{-1} corresponded to Al_2O_3 and WO_x [38, 39]. The peak at around 1060 cm^{-1} referred to (Ni,Co)O [40, 41], and the peak of 680 cm^{-1} appeared at elevated temperature indicated the existence of Co_3O_4 and $NiCr_2O_4$ [40, 42]. The peaks of Cr_xO_y also appeared at 360 cm^{-1}, 550 cm^{-1} [40, 43]. It can conclude that different kinds of metal oxides (including Al, Ni, Cr, Co, and W) were generated at elevated temperature. However, the metal oxides have different effects on the tribological behavior of the SP-NBSC superalloy. Specifically, Al_2O_3 had high hardness and strength, which acted as the main supporting point during the sliding wear, and therefore increased the anti-wear properties [28, 44]. The oxides of Cr, such as Cr_2O_3, were also beneficial to the reduction of friction and wear [17, 29, 45, 46]. Besides, the friction-induced Co-based and W-based oxides exhibited low shear strength, which contributed to the low COF [21, 30, 47]. NiO was also proved to be an effective solid lubricant, however, NiO had poor mechanical properties and promoted the abrasive wear [48]. In all, the synergistic effects of these metal oxides result in the decreased COF and wear rate of the SP-NBSC superalloy at elevated temperature. At room temperature, although friction-induced heat also caused the surface oxidation, the amount of the oxides was too small to improve the tribological performance of the SP-NBSC superalloy.

3.4 Cross-sectional Morphology

High temperature promoted the formation of the glaze-layer, which was composed of different metal oxides and contributed to the prominent tribological behavior of the SP-NBSC superalloy. The cross-sectional morphology beneath the wear track was analyzed using SEM to investigate the microstructure of the glaze-layer, as shown in Fig. 10. It can be observed that the two-layer structure formed after the high-temperature friction test, a plastic deformation layer was generated, the γ/γ' microstructures were seriously distorted due to the high contact stress. Above the deformation layer, there was a glaze-layer, which was originated from the compacting and sintering of wear debris. The glaze-layer can prevent the direct contact between the friction pair, and contribute to the low COF and wear rate due to the low shear strength of the metal oxides. However, no glaze-layer was formed at room temperature, it was because that the weak oxidation cannot provide enough oxides to form a continuous film, and the initially formed film will be continuously

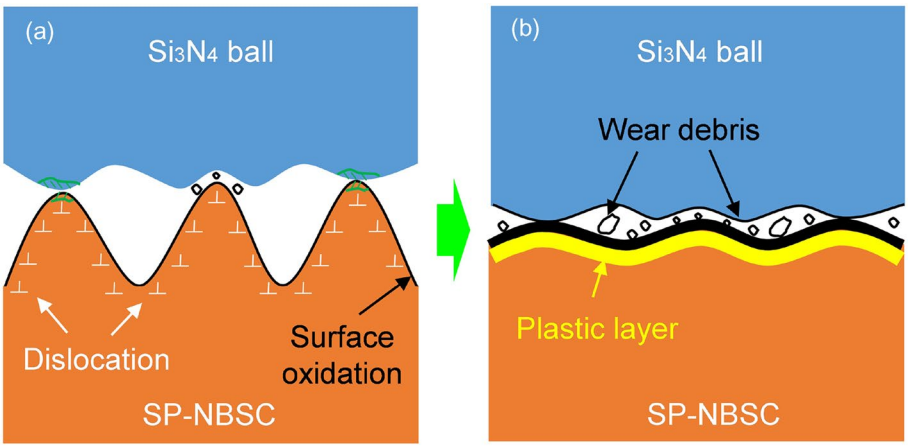

Fig. 11 The schematic of wear mechanism for SP-NBSC superalloy at high temperature. **a** Running-in period and **b** steady wear period

destroyed by the large frictional stress (Fig. 10a). In contrast, the tribo-layer formed at elevated temperature was dense, and the thicker tribo-layer could effectively protect the substrate (Fig. 10b–f). The γ/γ' microstructure beneath the glaze-layer was more distorted at 700 ℃ than that at 600 ℃, which may be induced by the degradation of the mechanical properties at higher temperature. When the test temperature was 600 ℃, both the thickness of the glaze-layer and plastic layer increased with the increase of the normal load. On the one hand, large normal load resulted in high contact stress and promoted the plastic deformation of the substrate. On the other hand, wear debris was easily generated and compacted on the specimen surface, which will promote the formation of the thicker glaze-layer.

3.5 Wear Mechanism

According to the above analyses, the wear mechanism of the SP-NBSC superalloy at high temperature was proposed (Fig. 11). The wear process of the SP-NBSC superalloy can be divided into two periods, i.e., the running-in period and steady wear period. During the running-in period, multiple rough peaks of the specimen surface were in contact with the Si_3N_4 ball, and the actual stress will be higher compared with the AS-NBSC superalloy due to the increased surface roughness of the SP-NBSC superalloy. Then, the surface material was worn off due to the large frictional stress and formed wear debris (Fig. 11a). At the same time, the friction-induced heat and high-temperature environment caused the surface oxidation. With the continuous friction, the surface oxidation and wear intensified, and a part of the wear debris accumulated and be trapped between the friction pair. The trapped wear debris would be sintered and compacted on the surface and form a glaze-layer (Fig. 11b). The glaze-layer was composed of different kinds of metal oxides (including Al, Ni, Cr, Co, and W), which prevented the direct contact of the friction pair. Furthermore, these oxides had good anti-wear and anti-friction properties, thereby improving the tribological performance under high-temperature conditions [14, 28, 30, 49].

The tribological performances of the SP-NBSC superalloy depended on the applied normal load and test temperature during the friction process, which led to the difference in wear mechanism. At room temperature, there was weak oxidation in the contact region, no glaze-layer was formed to protect the substrate, and the main wear mechanism was adhesion wear and abrasion wear. When the test temperature increased to 600 ℃ and above, severe oxidative wear occurred, and a glaze-layer was formed on the surface of the SP-NBSC superalloy due to the sintering and compacting of wear debris. The formed glaze-layer could avoid the direct contact of the friction pair and effectively reduce friction and wear. However, the wear mechanism under high temperature conditions was not exactly the same. At 600 ℃, both the adhesive wear and abrasive wear existed during the friction process, but the abrasive wear became prominent as the normal load decreased. When the test temperature increased to 700 ℃, the main wear mechanism was abrasive wear and oxidative wear, which may be attributed to the different composition of the formed glaze-layer.

4 Conclusion

The tribological behavior of the SP-NBSC superalloy has been investigated when sliding against the Si_3N_4 ball. The effects of temperature and applied normal load on the friction and wear were probed, and the wear mechanism of the SP-NBSC superalloy has also been revealed by analyzing the morphology and chemical composition of the wear track. The main conclusions of this work can be summarized as follows:

1) Shot-peening treatment increased the surface hardness of the NBSC superalloy by about 48.9%, and the surface roughness was more than ten times that of the AS-NBSC superalloy. Since the competing effects of the high hardness and large roughness on the tribological behavior, there were no significant differences in COF and wear rate between the SP-NBSC superalloy and the AS-NBSC superalloy.
2) The averaged COF of the SP-NBSC superalloy was about 0.62 at room temperature with a constant normal load of 20 N, which was almost twice those at 600 ℃ (COF = 0.34) and 700 ℃ (COF = 0.33). The wear rate showed a similar trend with temperature, which decreased drastically from 11.21×10^{-8} mm^3/(N·mm) at room temperature to 3.07×10^{-8} mm^3/(N·mm) at 600 ℃ and 3.24×10^{-8} mm^3/(N·mm) at 700 ℃. In addition, the larger normal load was beneficial to reducing COF, and the averaged COF decreased from 0.44 to 0.33 when the applied normal load varied from 10 to 20 N. However, the wear rates did not change significantly, which were 2.90 and 2.85×10^{-8} mm^3/(N·mm) when the applied normal load was 10, 15 N, respectively.
3) Friction-induced heat and high-temperature environment promoted the surface oxidation during the friction process. Under the action of high contact stress and frictional stress, severe wear occurred and a large amount of wear debris were generated, which will be sintered and compacted to form a glaze-layer on the surface. The glaze-layer was mainly composed of metal oxides of aluminum, nickel, chromium, cobalt, and tungsten, which contributed to the low COF and wear rate.

Acknowledgements This work was supported by National Natural Science Foundation of China (52105154 and 51975471), National Science and Technology Major Project (2017-VIII-0003-0114), China Postdoctoral Science Foundation (2022M711777), and Natural Science Foundation of Shanghai (21ZR1469300).

Declarations

Competing Interests The authors declare that we have no known competing financial interests or personal relationships that could have appeared to influence the work reported in this paper.

References

1. Lewis, R., Dwyer-Joyce, R.: Combating automotive engine valve recession. Tribol. Lubr. Technol. **59**, 48–51 (2003)
2. Prakash, P., Duraiselvam, M., Natarajan, S., Balamurugan, K.G.: Effect of laser surface texturing on wear resistance of nickel based superalloy. Ind. Lubr. Tribol. **71**, 842–850 (2019)
3. Sun, S., Li, L., He, K., Yue, Z., Yang, W., Yu, Z.: Fretting fatigue damage mechanism of Nickel-based single crystal superalloys at high temperature. Int. J. Mech. Sci. **186**, 105894 (2020)
4. Sun, S., Li, L., Yue, Z., Yang, W., He, K., Li, S.: Fretting fatigue failure behavior of Nickel-based single crystal superalloy dovetail specimen in contact with powder metallurgy pads at high temperature. Tribol. Int. **142**, 105986 (2020)
5. Tan, Z.H., Wang, X.G., Du, Y.L., Duan, T.F., Yang, Y.H., Liu, J.L., et al.: Temperature dependence on tensile deformation mechanisms in a novel Nickel-based single crystal superalloy. Mater. Sci. Eng. A **776**, 138997 (2020)
6. Chen, Y., Jiang, C.: Effect of shot peening on surface characteristics of Ni-based single-crystal superalloy. Mater. Trans. **54**, 1894–1897 (2013)
7. Wang, X., Xu, C., Hu, D., Li, C., Liu, C., Tang, Z.: Effect of ultrasonic shot peening on surface integrity and fatigue performance of single-crystal superalloy. J. Mater. Process. Technol. **296**, 117209 (2021)
8. Yan, W., Fang, L., Sun, K., Xu, Y.: Effect of surface work hardening on wear behavior of Hadfield steel. Mater. Sci. Eng. A **460–461**, 542–549 (2007)
9. Kubler, R., Berveiller, S., Bouscaud, D., Guiheux, R., Patoor, E., Puydt, Q.: Shot peening of TRIP780 steel: Experimental analysis and numerical simulation. J. Mater. Process. Technol. **270**, 182 (2019)
10. Mitrovic, S., Adamovic, D., Zivic, F., Dzunic, D., Pantic, M.: Friction and wear behavior of shot peened surfaces of 36CrNiMo4 and 36NiCrMo16 alloyed steels under dry and lubricated contact conditions. Appl. Surf. Sci. **290**, 223–232 (2014)
11. Dancer, C.E.J., Yahya, N.A., Berndt, T., Todd, R.I., de Portu, G.: Effect of residual compressive surface stress on severe wear of alumina–silicon carbide two-layered composites. Tribol. Int. **74**, 87–92 (2014)
12. Zammit, A., Abela, S., Wagner, L., Mhaede, M., Grech, M.: Tribological behaviour of shot peened Cu–Ni austempered ductile iron. Wear **302**, 829–836 (2013)
13. Fridrici, V., Fouvry, S., Kapsa, P.: Effect of shot peening on the fretting wear of Ti–6Al–4V. Wear **250**, 642–649 (2001)
14. Rynio, C., Hattendorf, H., Klöwer, J., Eggeler, G.: The evolution of tribolayers during high temperature sliding wear. Wear **315**, 1–10 (2014)
15. Meng, Y., Xu, J., Jin, Z., Prakash, B., Hu, Y.: A review of recent advances in tribology. Friction. **8**, 221–300 (2020)
16. Stott, F.H.: High-temperature sliding wear of metals. Tribol. Int. **35**, 489–495 (2002)
17. Stott, F.H., Lin, D.S., Wood, G.C.: The structure and mechanism of formation of the 'glaze' oxide layers produced on nickel-based alloys during wear at high temperatures. Corros. Sci. **13**, 449–469 (1973)
18. Jiang, J., Stott, F.H., Stack, M.M.: The effect of partial pressure of oxygen on the tribological behaviour of a nickel-based alloy, N80A, at elevated temperatures. Wear **203–204**, 615–625 (1997)
19. Bayata, F., Alpas, A.T.: The high temperature wear mechanisms of iron-nickel steel (NCF 3015) and nickel based superalloy (inconel 751) engine valves. Wear **480–481**, 203943 (2021)
20. Lawen, J.L., Jr., Calabrese, S.J., Dinc, O.S.: Wear resistance of super alloys at elevated temperatures. J. Tribol. **120**, 339–344 (1998)
21. Stoyanov, P., Dawag, L., Goberman, D.G., Shah, D.: Friction and wear characteristics of single crystal ni-based superalloys at elevated temperatures. Tribol. Lett. (2018). https://doi.org/10.1007/s11249-018-0994-1
22. Rynio, C., Hattendorf, H., Klöwer, J., Eggeler, G.: On the physical nature of tribolayers and wear debris after sliding wear in a superalloy/steel tribosystem at 25 and 300°C. Wear **317**, 26–38 (2014)
23. Wood, P.D., Evans, H.E., Ponton, C.B.: Investigation into the wear behaviour of Tribaloy 400C during rotation as an unlubricated bearing at 600°C. Wear **269**, 763–769 (2010)
24. Blau, P.J.: Elevated-temperature tribology of metallic materials. Tribol. Int. **43**, 1203–1208 (2010)
25. Li, L., He, K., Sun, S., Yang, W., Yue, Z., Wan, H.: High-temperature friction and wear features of Nickel-based single crystal superalloy. Tribol. Lett. (2020). https://doi.org/10.1007/s11249-020-1266-4
26. Dreano, A., Fouvry, S., Sao-Joao, S., Galipaud, J., Guillonneau, G.: The formation of a cobalt-based glaze layer at high temperature: a layered structure. Wear **440–441**, 203101 (2019)
27. Hager, C.H., Sanders, J., Sharma, S., Voevodin, A., Segall, A.: The effect of temperature on gross slip fretting wear of cold-sprayed nickel coatings on Ti6Al4V interfaces. Tribol. Int. **42**, 491–502 (2009)
28. Aouadi, S.M., Gao, H., Martini, A., Scharf, T.W., Muratore, C.: Lubricious oxide coatings for extreme temperature applications: a review. Surf. Coat. Technol. **257**, 266–277 (2014)
29. Korashy, A., Attia, H., Thomson, V., Oskooei, S.: Fretting wear behavior of cobalt—based superalloys at high temperature—a comparative study. Tribol. Int. **145**, 106155 (2020)
30. Viat, A., Dreano, A., Fouvry, S., De Barros Bouchet, M.-I., Henne, J.-F.: Fretting wear of pure cobalt chromium and nickel to identify the distinct roles of HS25 alloying elements in high temperature glaze layer formation. Wear **376–377**, 1043–1054 (2017)
31. Huang, C., Zou, B., Liu, Y., Zhang, S., Huang, C., Li, S.: Study on friction characterization and wear-resistance properties of Si3N4 ceramic sliding against different high-temperature alloys. Ceram. Int. **42**, 17210–17221 (2016)
32. Feng, K., Shao, T.: The evolution mechanism of tribo-oxide layer during high temperature dry sliding wear for nickel-based superalloy. Wear **476**, 203747 (2021)
33. Unal, O., Varol, R.: Surface severe plastic deformation of AISI 304 via conventional shot peening, severe shot peening and repeening. Appl. Surf. Sci. **351**, 289–295 (2015)
34. Liu, Y., Liskiewicz, T.W., Beake, B.D.: Dynamic changes of mechanical properties induced by friction in the Archard wear model. Wear **428–429**, 366–375 (2019)

35. Liskiewicz, T., Kubiak, K., Comyn, T.: Nano-indentation mapping of fretting-induced surface layers. Tribol. Int. **108**, 186–193 (2017)
36. Everitt, N.M., Ding, J., Bandak, G., Shipway, P.H., Leen, S.B., Williams, E.J.: Characterisation of fretting-induced wear debris for Ti-6Al-4 V. Wear **267**, 283–291 (2009)
37. Lai, P., Gao, X., Tang, L., Guo, X., Zhang, L.: Effect of temperature on fretting wear behavior and mechanism of alloy 690 in water. Nucl. Eng. Des. **327**, 51–60 (2018)
38. Chua, Y.T., Stair, P.C., Wachs, I.E.: A comparison of ultraviolet and visible Raman spectra of supported metal oxide catalysts. J. Phys. Chem. B **105**, 8600–8606 (2001)
39. Ozkan, E., Lee, S.-H., Tracy, C.E., Pitts, J.R., Deb, S.K.: Comparison of electrochromic amorphous and crystalline tungsten oxide films. Sol. Energy Mater. Sol. Cells **79**, 439–448 (2003)
40. Kim, J.H., Hwang, I.S.: Development of an in situ Raman spectroscopic system for surface oxide films on metals and alloys in high temperature water. Nucl. Eng. Des. **235**, 1029–1040 (2005)
41. Mironova-Ulmane, N., Kuzmin, A., Steins, I., Grabis, J., Sildos, I., Pärs, M.: Raman scattering in nanosized nickel oxide NiO. J. Phys. **93**, 012039 (2007)
42. Rashad, M., Rüsing, M., Berth, G., Lischka, K., Pawlis, A.: CuO and Co3O4 nanoparticles: synthesis, characterizations, and Raman spectroscopy. J. Nanomater. **2013**, 1–6 (2013)
43. Monnereau, O., Tortet, L., Grigorescu, C., Savastru, D., Iordanescu, C., Guinneton, F., et al.: Chromium oxides mixtures in PLD films investigated by Raman spectroscopy. J. Optoelectron. Adv. Mater. **12**, 1752 (2010)
44. Fernandez, J.E., Rodriguez, R., Wang, Y., Vijande, R., Rincón, A.: Sliding wear of a plasma-sprayed Al2O3 coating. Wear **181–183**, 417–425 (1995)
45. Khajuria, G., Wani, M.F.: High-temperature friction and wear studies of nimonic 80A and nimonic 90 against nimonic 75 under dry sliding conditions. Tribol. Lett. (2017). https://doi.org/10.1007/s11249-017-0881-1
46. Scharf, T.W., Prasad, S.V., Kotula, P.G., Michael, J.R., Robino, C.V.: Elevated temperature tribology of cobalt and tantalum-based alloys. Wear **330–331**, 199–208 (2015)
47. Geng, Z., Li, S., Duan, D.L., Liu, Y.: Wear behaviour of WC–Co HVOF coatings at different temperatures in air and argon. Wear **330–331**, 348–353 (2015)
48. Attia, M.H., de Pannemaecker, A., Williams, G.: Effect of temperature on tribo-oxide formation and the fretting wear and friction behavior of zirconium and nickel-based alloys. Wear **476**, 203722 (2021)
49. Hamdy, M.M., Waterhouse, R.B.: The fretting wear of Ti-6Al-4v and aged inconel 718 at elevated temperatures. Wear **71**, 237–248 (1981)